IONOMERS

1. Introduction

Polymers containing ions can be classified into two major families; polyelectrolytes and ionomers. In the case of the polyelectrolytes, the ion content is very high, eg, every repeat unit of the polymer has pendent ionic groups, and, thus, the polyelectrolytes are generally water soluble. On the other hand, the ionomers are used to define thermoplastic polymers, which contain a small amount of ionic groups (<15 mol%) in a matrix of low dielectric constants. The chemical structures of ionomers are shown in Fig. 1, where PSMA Na is poly(styrene-*co*-sodium methacrylate), NaSPS = sodium *p*-carboxylated polystyrene, Na-EMAA = sodium-neutralized ethylene-*co*-methacrylate, PTFE = polytetrafluoroethylene.

Historically, the word ionomer was first coined in 1965 (1), when it was used to describe a class of ionic thermoplastics consisting of ethylene and partly neutralized methacrylic acid units. Later, it was recognized that sometimes the ionomers (eg, polyacryamide ionomers) in solution showed polyelectrolyte behavior. Thus, another definition was proposed by Eisenberg and Rinaudo (2); if the bulk properties of polymers were governed by ionic interactions in ionic aggregates, the polymers would be classified as ionomers. When polymers are dissolved in solvents of high dielectric constants and the solution properties are governed by electrostatic interactions over a distance longer than typical molecular dimensions, the polymers are polyelectrolytes.

In the 1950s, it was found that the properties of elastomers could be changed significantly by the introduction of carboxylate ionic groups to the non-ionic elastomers (3). Since then, the introduction of ionic groups to non-ionic polymers has been used as a powerful tool for the modification of polymer properties. The typical examples of the effects of ionic interactions on the properties of ionomers can be found in the studies on glass-transition temperatures, mechanical properties, transport properties, and melt viscosities (4–6).

For example, the glass-transition temperatures (T_g) of poly(phosphoric acid), $(HPO_3)_x$, increases from -10 to 280°C, and to 520°C upon the neutralization of the acid groups with Na^+ and Ca^{2+}, respectively (7). This indicates that the ionization as well as ionic interactions between anions and cations are surely responsible for the increase in the T_g.

To envisage the mechanical properties of ionomers, the storage modulus (E') and loss tangent (tan δ) of PSMANa ionomers are shown in Fig. 2 as a function of temperature. It is seen that the modulus curve changes significantly with ion contents. For example, at 200°C polystyrene shows viscous flow behavior, while the 5.4 mol% ionomer exhibits a rubbery modulus of $\sim 10^{6.3}$ Pa; for the 21.6 mol% ionomer, the modulus value at the same temperature is a glassy modulus of $\sim 10^{8.8}$ Pa. This is due to an increase in the T_g of the ionomer, in part. For the ionomers of intermediate ion contents, the modulus changes from a glassy modulus, through a T_g, through a "ionic" plateau, through another glass transition, through a rubbery plateau, to a modulus for flow as the temperature increases. The T_g at low temperatures is known to be associated with the chain relaxation of ion-poor matrix regions, and the T_g at high temperatures is related to the chain relaxation and ion-hopping occurred in ion-rich clustered

regions (9,10). The plateau-like modulus curve between the two T_gs, ie, ionic plateau, is not seen in the ionomers of very low or very high ion contents and is due to the presence of ionic aggregates. With increasing ion content, the ionic plateau shifts to higher modulus values. In the case of loss tangent peaks, the two peaks shift to higher temperatures as the ion content increases. It is also seen that the size of the low temperature peak, ie, matrix peak, decreases, while that of the high temperature peak, ie, cluster peak, increases with increasing ion content. It is noteworthy that the relative sizes of the two loss tangent peaks of the PSMANa ionomers are directly related to the relative amount of the matrix and cluster regions (11,12). Thus, the trends shown in the relative peak sizes of the PSMANa ionomers (Fig. 3) indicate that at low ion contents the matrix phase is dominant, while at high ion contents the cluster phase becomes a dominant phase. In the case of the ionomer containing 5.4 mol% of ions, the relative sizes of the two loss tangent peaks are seen to be the same, illustrating that a comparable amount of high T_g material is present in the matrix of low T_g material (8). This suggests that the 5.4 mol% ionomer resembles a phase-separated blend.

In regard to the transport properties of ionomers, above a certain ion content, the ionic groups of the perfluorosulfonate and perfluorocarboxylate ionomer films in water become hydrated, resulting in the formation of water channel, in which ionic domains contain water (13,14). The formation of percolative water channel allows the ionomers high conductance. Similar trends can also be found in methyl methacrylate- and styrene-based ionomer films immersed in water (15,16).

The increasing melt viscosity of ionomers is another example of the striking effects of ionic interactions on the polymer properties. The melt viscosity of polystyrene homopolymer is $\sim 4 \times 10^3$ poise at 220°C. However, at an ion content of 3 mol%, the melt viscosity of para-carboxylated polystyrene (CPS) ionomer increases to 7×10^5 P, while that of SPS ionomer increases further to 9×10^8 P (17). As expected, the melt viscosity also increases with increasing ion content (17).

The above examples show that the polymer properties can be changed significantly through the ionic interactions and ion aggregation.

2. Characterization

2.1. Ionic Aggregates and Morphology of Ionomers. *Scattering and X-ray Absorption Studies.* In 1970, Eisenberg proposed that ionic groups of a polymer, the dielectric constant of which is low, form aggregates, termed multiplets (18). Since the ionic groups usually have high atomic numbers, the ionic aggregates act as the scattering centers of a high electron density (19). Thus, the morphology of the ionic aggregates has been investigated using a small-angle X-ray scattering technique (19–41). In small-angle X-ray scattering profiles for random ionomers, a broad scattering peak in the q ($= 4\pi \sin\theta/\lambda$) range from $\sim$0.5 to 3.0 nm^{-1} and a small-angle upturn at $q < 0.3$ nm^{-1} are usually observed (see Fig. 4). Since the appearance of the first article on the "ionomer" peak of the ethylene ionomer (19,20), a very wide range of morphology

studies has confirmed the existence of the ionomer peak in most ionomers, at least under some conditions. However, the interpretation of this ionomer peak is sometimes conflicting, which will be discussed below.

According to the para-crystalline lattice model based on the small-angle X-ray scattering data (21), the ionomer small-angle X-ray scattering peak is attributed to the contrasts of electron densities of the ionic aggregates and the hydrocarbon phase; thus, the peak position is thought to be related with the distance between ionic aggregates. In this model, the scattering centers are considered as points on a para-crystalline lattice. In a liquid-like interface model, so-called the Hard-sphere model proposed by Yarusso and Cooper (25), the multiplets are assumed to have liquid-like order and the distance of closest approach is governed by the thickness of a layer containing polymer chains on the surface of each multiplet. When the modified hard-sphere model was used to analyze the small-angle X-ray scattering peak at $2\theta = \sim 3.1^\circ$ of the Na-EMAA ionomers (5.4 mol% of ion content and 82% neutralization), the diameter of the aggregates was calculated to be $\sim$1.4 nm (39). In addition, the distance between ionic aggregates at their closest approach and the number of ionic aggregates changed upon the melting of crystalline regions and T_g of the EMAA and PSMANa ionomers, respectively (39). In another study, it was found that when the degree of neutralization increased, the small-angle X-ray scattering peak of EMAA ionomer shifted to lower angles only slightly. Thus, it was suggested that the size of the ioni aggregates (radius $= \sim 0.6$ nm), containing 7–12 ion pairs, did not change with changing the degree of ionization (40).

In the Core-shell model, however, MacKnight and co-workers. suggested that an ionic core of $\sim$1.0-nm radius is surrounded by a shell of hydrocarbon materials containing no ionic groups, which, in turn, is surrounded by a shell of polymeric materials of higher ion content (23). Thus, the distance between the two ion-rich regions, ie, the ionic core and the outer ionic shell, gives rise to the ionomer small-angle X-ray scattering peak. The parameters obtained from the fitting of the three models to the small-angle X-ray scattering data of ionomers have been found to be different each other. This indicates that the interpretation of the small-angle X-ray scattering data is model dependent. Besides small-angle X-ray scattering studies, a small-angle neutron scattering technique was also employed to investigate the interphase morphology of ionomers as well as chain conformation (41–46).

An extended X-ray absorption fine structure (XAFS) technique was used to determine the structure of atoms around the neutralizing cation in multiplets (47–54). For example, in the plots of radial structure function of Zn-EMAA ionomer (11 wt% MAA units), as the degree of neutralization increased, the position of the second-shell extended XAFS peak at $R_f = 0.29$ nm shifted to a lower value with increasing its height (53). This implies that the relative size of the multiplet of the Zn-EMAA ionomer increases by increasing the degree of neutralization. In addition, for the Zn-EMAA ionomer, four oxygen atoms were found to surround the zinc cation; the average distance between oxygen and zinc was $\sim$0.195 nm. The arrangement of the atoms did not change with degree of neutralization. In the case of Na-EMAA ionomers, however, the arrangement of atoms around Na was found to change significantly with the degree of neutralization; this revealed that the degree of neutralization affected

the three-dimensional (3D) arrangement of atoms in multiplets of Na the system (54). It was also found that the change in the arrangement of atoms of the Zn-EMAA ionomer was not noticeable below the melting temperature of polyethylene. These results indicated that the crystallinity and types of neutralizing agents influenced the conformation of ionic aggregates of EMAA ionomers strongly.

Electron Microscopic Studies. Since the interpretation of the electron microscopic images of ionomers is model independent, the electron microscopy provides various valuable information, including the size, shape, size and shape variation, and distribution of ionic aggregates in a matrix (55–61). In one of early studies, it was found that a high voltage electron microscopy image of the ultrathin films of the ZnSPS ionomer rapidly cast from solution onto copper grids showed ionic domains irregularly distributed throughout the polymer matrix (56). The shape of the ionic domain was more or less spherical, and the size was $\sim$3 nm. Recently, a scanning transmission electron microscopy technique has been employed to investigate the ionomer morphology (57–61). For example, it was observed that spherical aggregates of $\sim$2 nm in diameter were randomly distributed in the matrix of semicrystalline Zn-EMAA ionomers (57,58). In the case of the amorphous Zn-sulfonated polystyrene (ZnSPS) (59) and Cs-neutralized PSMAA ionomers (60), macrophase separation of the ion-rich regions from ion-poor regions was observed; the shapes of the ionic aggregates were found to be spheres and/or vesicles. It was also observed that the recrystalized Na-EMAA ionomer showed three different separated regions (61). The first regions do not have aggregates $>$1 nm, and the second regions contain spherical particles, whose sizes are in the range of $\sim$2–15 nm. The last regions possess larger aggregates, the sizes of which are in the range of $\sim$20–160 nm. In the case of the block ionomers, multiple morphologies have been observed using a transmission electron microscopy technique (62–64). The equilibrium, near-equilibrium, and nonequilibrium morphologies are spheres, rods, bicontinuous rods, bilayers, lamellae, vesicles, inverse bicontinuous rods, large compound micelles, aggregates of spheres, large rod-shaped compound micelles, large compound vesicles, and many others (64). At this point, it should be mentioned that very recent research has shown that the differences in sample preparation methods and the nature of the analytical techniques could make the ionomer morphology obtained from the interpretation of small-angle X-ray scattering data differ from that obtained from electron microscopic data (65). Thus, to obtain unified morphological picture of ionomers more thorough research is needed.

Atomic Force Microscopy. For the transmission electron microscopy study, the sample specimen has to be a very thin polymer film. However, for the morphological study using atomic force microscopy techniques, thin sections of the sample are not required. Furthermore, the resolution of recent tapping mode atomic force microscopy is found to be comparable to that of the transmission electron microscopy for crystalline lamellae on a polymer surface. In addition, the tapping mode phase imaging technique has an advantage; it can distinguish between the surface areas having different surface properties regardless of their topological nature. Thus, recently, the atomic force microscopy techniques were applied to investigate ionomer morphologies (66–69). In the case of the perfluoro-sulfonate cation exchange membranes, the tapping mode phase

images reveal that the sizes of the agglomerates of clusters, consisting of water molecules and ionic groups, are in the range of 5–30 nm (67). In the case of EMAA ionomers, under different tapping conditions, the ionic domains of the ionomers neutralized with Zn and Na are found to be mainly located in the "softer" amorphous regions than the crystalline regions (69).

Multiplets. The multiplet–cluster model, so-called Eisenberg-Hird-Moore (EHM) model, incorporates morphological features together with mechanical properties of amorphous random ionomers (9). In the model, the small-angle X-ray scattering peak is assumed to be related with interparticle scattering, as in the Cooper's model (25). The size of a multiplet, consisting of several ion pairs, is limited by a number of factors (18). A steric effect of the polymer chain segments adjoining ion pairs is one of main factors controlling the multiplet size. This effect gives an upper limit on the size of the multiplets because each ion pair is attached through a covalent bond directly to a polymer chain or to a spacer emanating from a polymer backbone, and most of the ionic groups reside inside of a multiplet, while the organic polymer segments must be outside of the multiplet.

The size of ion pair (27,70), the polarity of polymer matrix (7,71,72), the distance between an ionic group and a polymer backbone (10,25), the strength of ionic interactions (9,10), an ion content (9,10,28), and the number of ionic groups per ionic repeat unit (73,74) also affect the multiplet size. For example, small ion pairs attached to a relatively bulky chain backbone could form small ionic aggregates, while large ion pairs attached to a very flexible backbone lead to the formation of large ionic aggregates. When the polarity of the polymer matrix is high, the ionic groups are solvated, resulting in no ionic aggregates. If the distance between ionic groups and polymer backbone increased, the size of the ionic aggregates would increase because the ionic groups experience less steric hindrance when they form multiplets. This can be evidenced by the small-angle X-ray scattering results obtained from the styrene ionomer (7.5 mol% of ions), where an ionic group is attached to the para position of benzene ring through a flexible alkyl side chain (26). It was found that when the number of carbon atoms of the side chains increased from 2, to 6, and to 11, the calculated number of ion pairs per multiplet increased from 21 to 37, and to 60, respectively. The radius of the multiplet also increased linearly with increasing the side chain length from an extrapolated value of $\sim$0.4 nm for the cesium-methacrylate system to $\sim$1.1 nm for the ionomer containing the alkyl chain of 11 carbons. At this point, the relation between the multiplet size and the strength of ionic interaction is worth mentioning. In the cases of NaSPS and NaCPS ionomers, the strength of ionic interactions in the Na-sulfonate ion pairs is much stronger than that of the Na-carboxylate ion pairs. Thus, the number of the ionic groups per multiplet of the NaSPS ionomer is naturally larger than that of the NaCPS ionomer (9,10,75). This, in turn, results in the fewer multiplets in the NaSPS ionomer, compared to the NaCPS ionomer at a comparable ion content.

2.2. Reduced Mobility of Chains in Clusters. In the cases of PSMANa and NaSPS ionomers, two polymer chains come out from one ion pair because the ionic groups are attached to a polymer chain directly and through a benzene ring linkage, respectively. In the EHM model, the chains in the immediate vicinity of the multiplet are suggested to be restricted in their

mobility, with the effect of the chain mobility restriction becoming weaker as the distance between the polymer chain segments and the multiplet increases (9). The chain mobility restriction is due to the fact that the multiplet holds the polymer chains emanating from it tightly, and, thus, the mobility of the polymer chains is significantly lower than that of the polymer chains in non-ionic polymer matrix. In addition, bridging between neighboring multiplets through polymer chains is expected to put the polymer chains under tension, resulting in the low mobility of the chains. Furthermore, the crowding of polymer chains in the vicinity of the multiplet also decreases the chain mobility (76). A considerable amount of supportive evidence for the restricted mobility of polymer chains has been collected in the studies using various techniques including nuclear magnetic resonance, electron spin resonance, dielectric, and dynamic mechanical techniques (40,77–86).

In the EHM model, the thickness of the reduced mobility layer surrounding the multiplet is postulated to be of the order of the persistence length of the polymer chain [eg, ∼1.0 and 0.7 nm for polystyrene and poly(methyl methacrylate), PMMA, respectively]. Thus, the size of the reduced mobility region of a material including multiplets is <3.0 nm (see Fig. 5), which is too small for the reduced mobility regions to show its own glass transition. With increasing ion content, the number of multiplets increases, and the reduced mobility regions start overlapping. Consequently, the dimensions of the reduced mobility regions enlarge enough to exceed a threshold value for independent phase behavior. The presence of these large reduced mobility regions, called clusters, results in the appearance of a second T_g at much higher temperatures than the T_g for the non-ionic matrix phase. With increasing ion content further, the amount of cluster regions in the material increases, whereas that of the ion-poor matrix regions decreases. Eventually, the cluster regions become dominant and even continuous with increasing ion content.

3. Glass Transitions

At certain ion contents, amorphous random ionomers, eg, polystyrene-based ionomers, show two glass transitions (T_gs). As shown in Fig. 2, the non-ionic polystyrene (PS) homopolymer and the PSMANa ionomer containing 21.6 mol% of ions exhibit only one modulus drop as well as one loss tangent peak at ∼120 and at ∼320°C, which are the matrix and cluster loss tangent peaks for the PS and the PSMANa ionomer, respectively. Interestingly enough, the activation energies for the glass-transitions calculated using an Arrhenius equation with the data of frequencies and temperatures of the peak maximum are found to be comparable each other, ie, 520 kJ/mol for the polystyrene and 640 kJ/mol for the 21.6 mol% ionomer (8). In the case of the ionomers of intermediate ion contents, they show two modulus drops and two loss tangent peaks. The peak positions for the PSMANa system are shown in Fig. 6 as a function of ion content along with those obtained from various PS ionomers (8,10,73,87,88). Two glass transitions in some of PS-based ionomers have also been observed by using a differential scanning calorimeter (10,87,89–92), and by measuring the volume of ionomers as a function of temperature (93).

In an early study on the effect of the degree of neutralization on the T_g of semicrystalline EMAA ionomers, MacKnight and co-workers (94) found that the loss tangent peak at $\sim 0^\circ$C shifted to lower temperatures upon neutralization and, thus, suggested that the peak was associated with a β relaxation of polymer chains in the ion-depleted, amorphous branched polyethylene phase. Subsequently, Otocka and Kwei (95) observed that the T_g of ethylene-*co*-acrylate ionomers increased with increasing ion content. In the case of amorphous PSMANa ionomers, the increase in the matrix T_g with increasing ion content was found by Eisenberg and Navratil (96). They suggested that the increase in the matrix T_g is due to the fact that isolated multiplets and the surfaces of clusters would act as cross-links, which naturally leads to the increasing T_g. At this point, it should be noted that the matrix T_g does not always increase upon the ionization of acid form copolymers. For example, if the length of alkyl chain of alkyl ammonium-SPS ionomers were long enough, the matrix T_g would decrease with increasing ion content, since in that system the long alkyl chain acts as an internal plasticizer (97). Similar results were also found in styrene-vinylpyridinium alkyl halide random ionomers (98).

In the case of PSMANa ionomers of low ion contents, the cluster T_g is $\sim 60^\circ$C higher than the matrix T_g and increases almost in parallel with the matrix T_g (Fig. 6). By increasing ion content further, however, the cluster T_g shifts to higher temperatures more rapidly; thus, the cluster T_g of the 15 mol% ionomer becomes $\sim 110^\circ$C higher than the matrix T_g. At this point, it should be mentioned that whereas the mechanism of the matrix T_g of the ionomers is the same as that of non-ionic polymers, the mechanism of the cluster T_g is still rather ambiguous. At and above the cluster T_g, with sufficient thermal energy the bound ion pairs are thought to hop (or "diffuse") from one multiplet to another at a fast rate through the nonpolar polymer matrix (ie, so-called ion hopping) (8–10, 99–101). This allows the relaxation of stress in the polymer chain segments of the restricted mobility regions via the micro-Brownian motion of polymer chains. This chain relaxation, indeed, takes place simultaneously with the ion hopping at and above the cluster T_g of ionomers.

Since the strength of ionic interaction is directly related with the temperature for ion hopping, the type of ionic groups (ie, including the strength, size, oxidation number of ions as well as the number of ionic groups per ionic repeat unit) (9,10), indeed, affects the cluster T_g significantly. For example, the ionic interaction between Na-sulfonate ionic groups is stronger than that between Na-carboxylate ionic groups owing to the difference in the 3D arrangement of the cation and the anion (75), and, thus, the NaSPS ionomer needs higher temperature for the ions to hop than the PSMANa does (10). Therefore, the cluster T_g of the former ionomer is higher than that of the latter ionomer at a comparable ion content (Fig. 6) (10,75,102,103). At this point, note that the activation energies for ion hopping of the NaSPS system are generally lower than those of the PSMANa system despite the opposite trend in the strength of ionic interaction (8,10). This indicates that the strength of the ionic interaction is directly related with the cluster T_g, but not with the activation energies for ion hopping (8).

One of examples showing the effect of the size of ions on the cluster T_g can be found in the poly(styrene-*co*-*N*-methyl-4-vinylpyridinium iodide), PS-4VPMeI,

copolymers (27,104). In this system, with increasing ion content the matrix T_g is found to increase at a similar rate found in other PS-based ionomers. However, the cluster T_g is not observed, suggesting that the ionomers are unclustered materials. This result can be understood. The sizes of *N*-methyl vinylpyridinium cation and iodide anion are too large for strong ionic interactions, and, thus, the ionic groups do not form a sufficient number of multiplets. In addition, the relatively high T_g of the polystyrene matrix is also attributed to no clustering in this ionomer system.

At this point, note that the plasticization of polymers is effective for the decreasing T_g of the polymer. Thus, one can use the plasticization method to decrease the matrix T_g of ionomers. If the matrix T_g decreased sufficiently, more multiplets form, leading to the noticeable clustering in the ionomer system (27,71,105,106). Therefore, sometimes the unclustered ionomers can be converted into clustered materials through polar, nonpolar, or amphiphilic plasticization.

The effects of both the size and the oxidation number of ionic groups on the cluster T_g can be found in the poly(ethyl acrylate-*co*-acrylate), PEA, ionomer system (70). It is observed that the matrix and cluster T_g values increase relatively linearly with increasing ion content. In this case, the increasing rates of the matrix T_g do not change with the type of cations; they are only affected by the ion content. In the case of cluster T_gs, however, the increasing rates are influenced by the type of cations. According to a q/a (where q is a cation charge and a is a distance between the centers of an anion and a cation) relationship with electric force between charges, the T_g is proportional to the electrostatic work needed to separate the anion from the cation (107). Thus, the interaction between ions becomes stronger with decreasing the cation size and with increasing the oxidation number, leading to the higher cluster T_g.

When the ionic repeat unit has two ionic groups, eg, poly(styrene-*co*-itaconate) (73) and poly(styrene-*co*-citraconate) (88) ionomers, only a very weak cluster loss tangent peak (indicating weak clustering) is present at much higher temperature than the cluster T_g of well-clustered PSMANa ionomer; the weak cluster peak shifts to higher temperatures with increasing ion content. The weak clustering is probably due to the fact that the presence of two ion pairs in one ionic repeat unit is more effective in stiffening polymer chains, compared to the methacrylate ionomer. In addition, the higher cluster T_g is owing to the presence of two ion pairs in an ionic repeat unit, which makes ion hopping difficult and, thus, results in a higher cluster T_g. The morphological study of this ionomer reveals that as ion content increases more ionic groups participate in the formation of multiplets (73).

4. Properties

4.1. Styrene Ionomers. In the plot of modulus versus temperature (see Fig. 2), two inflection points are seen for the PSMANa ionomers of intermediate ion contents. The modulus values at a higher inflection point, ie, "ionic" modulus, are in the range of $\sim 10^{6.5}$–$10^{8.5}$ Pa, which increases with increasing ion content. The modulus values at a lower inflection point, ie, rubbery modulus, are more or

less constant at $\sim 10^{5.5}$ Pa. Since the ionomer shows many properties of filled materials, the increase in the modulus with ion contents, especially ionic modulus, can be related with a filler effect. With the volume fraction of clustered regions obtained from the relative areas under the two loss tangent peaks, the ionic modulus value can be calculated using the Guth equation, assuming that the filler effect is also operative for the ionomer system. Then, one could find that the Guth equation fits the experimental data for ionic modulus values of the PSMANa ionomers, up to ~3 mol% of ion content (~45 vol% of a clustered phase) (see Fig. 7) (8). This implies that clusters, not ionic aggregates, act as fillers in the temperature range between the matrix and cluster T_g values of the ionomers of low ion contents. It can also be suggested that the inversion from matrix-dominant materials to cluster-dominant materials with increasing ion content resembles the percolation of the clustering in ionomers (13). Thus, the ionic modulus of the PSMANa system is fitted with the equation dealing with the behavior of percolative materials. In Fig. 7, it is also seen that the percolation concept is indeed applicable for the clustering behavior of ionomers containing 5–10 mol% of ions, with the critical exponent of 1.3, which is very close to the universal value for conductivity percolation (~1.5) and critical volume fraction of ~0.64, which corresponds to 5.4 mol% of ions.

The effects of the type of ionic groups on mechanical properties of the PS-based ionomers are discussed in this section. Even though the related discussion has already been present, this discussion should be very useful for the readers to understand clearly the relationship between chemical structure–morphology–mechanical properties of various ionomers that will not be mentioned in this article. The storage moduli for the NaSPS and PSMANa ionomers containing ~5 mol% of ions are shown in Fig. 8 as a function of temperature. Two major differences are observed. First, the "ionic plateau" of the NaSPS ionomer, which is associated with clustering, is longer in length (meaning higher cluster T_g), but lower in modulus values (meaning lower degree of clustering) than that of the PSMANa ionomer. The higher cluster T_g of the NaSPS is due to the fact that the ionic interactions between the Na-sulfonate ionic groups are stronger than that between Na-carboxylate. For the lower ionic plateau of the NaSPS, two aspects should be considered simultaneously (10). The ion pairs of the NaSPS ionomer are located in the para position of the benzene ring, while those of the PSMANa ionomer are directly attached to the main chain. Thus, the distance between the ion pair and the main chain is longer for the NaSPS ionomer than for the PSMANa ionomer. Therefore, the ion pairs of the NaSPS ionomer experience less steric hindrance when they form ionic aggregates, compared to those of the PSMANa ionomer. As a result, the average size of the multiplets of the NaSPS ionomer is larger than that of the PSMANa ionomer. The second aspect is the strength of the ionic interactions. The ionic interactions between the Na-sulfonate ion pairs of the NaSPS ionomer are much stronger than those between the Na-carboxylate of the PSMANa ionomer. This stronger ionic interaction enlarges the average multiplet size of the NaSPS ionomer, compared to that of the PSMANa ionomer (10). At this point, the morphology and ionic modulus of NaCPS ionomer can be discussed as well. According to the above discussion, the average size of the multiplets of the three PS ionomers would decrease in the following order: NaSPS > NaCPS >

PSMANa. When the size of the multiplet is larger, the number of the multiplets is fewer, which, in turn, makes the distance between the multiplets longer. Thus, when one changes the ionomers from the PSMANa, through the NaCSP, and to the NaSPS ionomer, one finds that the small-angle X-ray scattering ionomer peak shifts to lower angles (meaning fewer scattering centers) with increasing intensity (meaning a larger multiplet) (9,10). This morphological picture implies that if the thickness of the restricted mobility regions surrounding multiplets were the same for the three PS ionomer systems, the total volume of restricted mobility regions, ie, degree of clustering, is the smallest for the NaSPS ionomer and the largest for the PSMANa ionomer. As a result, the ionic modulus related with the clustering degree should be lowest for the former ionomer system and highest for the latter ionomer system at an identical ion content. Needless to say, at a comparable ion content the modulus and T_g values (even the small-angle X-ray scattering peak position) for the NaCPS ionomer are in between those for the NaSPS and PSMANa ionomers (10).

For the stress relaxation results of the ionomers, it was found that when the individual curves of modulus versus time were shifted to make one master curve, the time–temperature superposition of the curves was applicable for the ionomers containing less than ~6 mol% of ions (108). However, above that ion content, the time–temperature superposition of the individual curves was found to fail. As the ion content of ionomers increases, the nature of the ionomer changes from a matrix-dominant material to a cluster-dominant material progressively (9). Thus, at a certain ion content, the percolation threshold for the connectivity of clustered regions occurs and is ~5.4 mol% for the PSMANa ionomer system, as mentioned before (8). Below that ion content, the continuous phase matrix regions are responsible for ionomer behavior, but above the percolation threshold, both the clustered and unclustered matrix regions are attributed to the ionomer properties. Thus, the time–temperature superposition is not applicable above the percolation threshold for the connectivity of the clustered regions. Note also that, at very high ion contents, the cluster regions, being a continuous phase, determine the ionomer properties.

The melt viscosity of the NaSPS ionomer (1.7 mol% of ions) obtained by freeze-drying a ionomer solution (4 wt%), ionomer concentration of which was above the coil overlap concentration (C^*), was found to be nearly an order of magnitude higher than that of the ionomer isolated by freeze-drying at 0.3 wt% ($< C^*$), ie, $\sim 7 \times 10^7$ P versus 7×10^6 P (109). This illustrates that the ion aggregation restrains the chains from being entangled. It was also observed that the viscosity of the ionomer freeze-dried from a 0.3 wt% ionomer solution increased with increasing time, but was still only one-fifth that of the ionomer prepared from a 4 wt% ionomer solution, indicating that entanglements evolve between polymer chains that were initially isolated.

4.2. Other Ionomers. Various ionomers based on polymers other than polystyrene have also been investigated extensively. Among them, the most well-known ionomers are based on polyethylene (PE) and PTFE, which are partly crystalline. Thus, the properties of those two ionomer systems are discussed very briefly. At this point, note that the crystallinity of the two ionomers makes the interpretation of experimental results difficult, compared to the amorphous ionomers such as styrene ionomers.

Polyethylene Ionomers. In 1965, the first commercialized ionomer, ie, an ethylene ionomer Surlyn, was introduced to the market. Since then, the properties and morphologies of the ionomers have been investigated extensively (1,19,20,39,40,53,54,58,69,94,99,110–115). The ethylene ionomers are well known for their excellence in flexibility, transparence, toughness, and melt processibility. The stress relaxation curves of Na-EMAA ionomer (8 mol% of MAA content and 47% of neutralization) are shown in Fig. 9 (99). The slow rate of stress relaxation and no drastic glass transition are seen. Even though, the shapes of the curves are different from those obtained from amorphous ionomers, the stress–relaxation results are very similar to those of some amorphous ionomers of very high ion content or highly crystalline non-ionic polymers. It is also found that one could not superimpose the individual curves with WLF type shift factors to construct a master curve, which indicates that more than one mechanism might be responsible for the relaxation of the material.

In the plots of decrement versus temperature, four peaks were observed (not shown here) (94). It was suggested that the first peak (γ) at ca. -120°C was possibly due to the crankshaft motion of short hydrocarbon segments in the amorphous phase. The second peak (β) in the temperature range of -20–0°C increased its height slightly with increasing the degree of neutralization, but the position remained more or less constant; these were also observed for the EMAA ionomers of various ion contents (111). Thus, the β peak was suggested to be related with a relaxation in the amorphous branched polyethylene phase having no ionic group. The third peak (β') in the temperature range of 0–50°C decreased its height with increasing the degree of neutralization; the peak position also did not change. Thus, this peak was proposed to be related with the micro-Brownian motion of polymer chains, occurring in the amorphous polymer having hydrogen bonds. The forth peak (α) at high temperatures ($>50^{\circ}$C) shifting to higher temperatures with increasing the degree of neutralization might be attributed to micro-Brownian motions of relatively large segments of polymer chain and related with the dissociation of the ionic aggregates. Later, it was found that when the degree of neutralization increased to relatively high, a new relaxation peak (α') peak at $\sim 50^{\circ}$C was observed, and the peak position was not changed with frequencies (112). Thus, it was speculated that the α' peak might be due to an order–disorder transition of ionic clusters.

In the study of the melt-rheology of the EMAA ionomers, it was observed that the ionomers showed Newtonian behavior at low shear rates (114). In addition, it was also found that the zero-shear viscosity was related with neutralization degree and was higher for the Zn-EMAA ionomers than for the Na-EMAA ionomers. However, the type of cations and degree of ionization did not affect the recoverable compliance, which implied that ionic aggregates do not bear stress during steady flow in the terminal zone for ionomer melts. Thus, it was suggested that the lifetimes of the ionic aggregates were much shorter than those of the relaxation time of the polymer chains in the terminal region. Later, in a parallel melt rheology and cation diffusion study, it was found that the ionization level very strongly affected the zero-shear viscosities of the EMAA ionomers, with only minor effect of the type of cations (101). The diffusivity of the cations through the ionomer matrix was also found to be inversely related to the melt viscosity of the ionomers. In addition, the type of cations

influenced the relaxation time of the polymer chains more strongly than the ion-hopping time, which was approximately five orders of magnitude shorter than the former; however, the two relaxations had similar activation energies. Since the melt rheological properties of ionomers might be much more practically important for producing ionomic thermoplastic elastomers, the interested readers are referred to a review dealing with the melt rheology of various ionomers, ie, Chapter 5 of Ref. (5).

Polytetrafluoroethylene Ionomers. Studies on the mechanical properties of perfluorosulfonate ionomers, eg, Nafion, have been carried out extensively (116–120). In the case of the precursor and the acid form polymers, the time–temperature superposition of stress relaxation curves could be applicable when the degree of crystallinity was relatively low (117). However, when the acid groups were converted to potassium salts, the time–temperature superposition was found to be applicable only above ∼180°C (116). In addition, the precursor, acid form, and ionomer samples did not show two step drops in the plots of modulus versus temperature, which was probably due to the crystallinity and the different morphology occurred in the ionomers, compared to styrene ionomers. In the study of the effect of crystallinity on the 10-s modulus, it was found that the modulus curve of the amorphous Nafion was similar except that the position of the curve was lower by ∼40°C, compared to the crystalline Nafion.

In the plots of the loss tangent versus temperature of the completely neutralized Cs ionomer, three peaks were observed at ∼215°C (α), 160°C (β), and −100°C (γ) (116). The α, β, and γ peaks were suggested to be attributed to the glass transition of polymer chains in clustered regions, to that in the matrix regions, and to local motions of CF_2 groups of the polymer main chains in noncrystalline regions, respectively. The α peak was found to shift to higher temperature with increasing degree of neutralization (118).

In the case of the perfluorocarboxylate ionomers, it was found that they absorbed far less amount of water than the perfluorosulfonate ionomers (121). In addition, two more dynamic mechanical loss peaks (β′ and γ′) were observed. Compared to three peaks for the perfluorosulfonate ionomers. The mechanism for the relaxation associated with β′ peak in the temperature range between α and β transitions was not identified, and the γ′ peak between temperatures for the β and γ relaxations was assigned to local motions of the polar side groups in the matrix.

Because the description of the properties and morphologies of all the ionomer families is not possible here, only a few of more extensively studied ionomers will be named here. These include block ionomers (122–127), telechelic ionomers (41,128–133), star ionomers (134–138), polyurethane ionomers (139–141), ionenes (142–144), ethyl (or butyl) acrylate zwitterionomers (145,146), ethyl acrylate ionomers (70,74,147–149), methyl methacrylate ionomers (71,105,150,151), and liquid crystalline ionomers (152–158). It should also be mentioned that recently the investigation on the solution properties of ionomers becomes of great importance; especially, the self-assembly of random and block ionomers in solution requires the understanding of the behavior of ionomers in solution. Thus, readers who are interested in the solution properties of ionomers should refer to other review articles (159–162).

4.3. Ionomer Blends. In view of the significant improvement in material properties that can be achieved in polymer blends over their individual components, it is not surprising that extensive efforts have been made to study miscibility in polymers (163–166). These studies have been performed not only in industrial laboratories, but also in a number of academic laboratories, with the aim of both improving properties and understanding the fundamental relationships between polymer miscibility, the properties of the individual materials, and the properties of blends.

Regarding the thermodynamics of mixing; the entropy of mixing of polymers is very small because of very high molecular weights of the polymers. Thus, even a very small positive enthalpy change caused by unfavorable mixing makes most polymer pairs immiscible. In the case of miscible polymer pairs, sometimes one finds specific interactions between the polymer pairs, which reduce the enthalpy change even to negative values. Therefore, the addition of specific additives to polymer pairs or the physical and chemical modifications of the polymer pairs are required for miscibility enhancement. The first two methods include the addition of interfacial agents such as emulsifiers, reactive processing, high stress shearing, cocross-linking, the formation of interpenetrating networks, and others (167–170). The last method, ie, chemical modification, is the introduction of interacting groups to polymer pairs. The interactions include hydrogen bonding (171–178), acid–base interactions (179), ionic interactions, dipole–dipole interactions (180–183), and the formations of donor–acceptor complexes (184) or charge-transfer complexes (185–188). Since the early 1980s, the introduction of ionic interactions to non-ionic polymers have received considerable attention as a tool for the enhancement of polymer miscibility. An example of this type of miscibility improvement can be found in the formation of homogeneous polyelectrolyte complexes consisting of a polyanion and a polycation (179,189–195). To date, innumerable papers dealing with ionomer blends have been published, thus the following section is to introduce readers to a simple description of the types of ionomer blends, rather than an encyclopedic coverage of the topic. Interested readers are referred to reviews on the ionomer blends (196–199).

Various types of ionic interactions can be used to enhance polymer miscibility. Figure 10 shows the different types of the interactions. A simple ion–ion interaction, which arises between groups such as *N*-methylpyridinium and benzenesulfonate, is the first candidate (Fig. 10**a**). For example, ionomer blends having this type of interaction can be obtained by mixing a first copolymer containing sulfonic acid neutralized with a large cation, such as an alkyl ammonium ion, and a second copolymer containing pendent pyridinium ions with a large counteranion, such as iodide (200–202). In this case, the micro-ion, alkyl ammonium iodide, still remains in a solvent, and the polymer blend precipitates as a gel because of strong interactions between ionic groups. Another example of ion–ion interactions can be found in ionomer blends using proton transfer between two different polymers (Fig. 10**b**). For example, one polymer contains vinylpyridine units, and the other has a pendent sulfonic acid (203). Then, upon mixing of the two polymers protons can transfer from the sulfonic acid to the vinylpyridine, resulting in a cationic pyridinium polymer chain converted from the chain containing the pyridine and an anionic sulfonate polymer chain

from the chain containing the sulfonic acid. Thus, ion–ion interactions between the two polymers can take place. In this blend, the elimination of micro-ions is not required; hydrogen bonding between the pyridinium cation and the sulfonate anion becomes an additional benefit.

An ion pair–ion pair interaction can also be used as one of the tools for miscibility enhancement (202,204,205). When a sodium carboxylate ion pair attached to one polymer chain interacts with a quaternary ammonium halide (205) (Fig. 10**c**) [or the same sodium carboxylate (204) (Fig. 10**d**)] ion pair on the other polymer, the miscibility of blends can be achieved. In this blend, the microcounter-ions remain in the blend and, in some cases, would crystallize in the form of microcrystals, which act as filler.

The third and fourth types of ionic interactions used in ionomer blends are ion–dipole interactions involving the alkali and alkaline earth metal cations (206–211), and ion coordination with the presence of transition metal ions (212–214). For example, the lithium cation from the PSMALi ionomer can interact with a polar polymer, such as poly(ethylene oxide), PEO, through ion–dipole interactions (Fig. 10**e**) (206). An example of the ionomer blend using ion coordination is a blend of a poly(ethyl acrylate-*co*-4-vinylpyridine) copolymer and a Zn-SPS ionomer (Fig. 10**f**) (214). In that the zinc cation exists in tetra-coordinated environment, involving two pyridine groups and two sulfonate groups together. Note that the interactions between zinc and pyridine are coordinate covalent bonding, rather than simple anion–cation interactions. The ion-coordination interactions are very strong and result in very effective miscibility enhancement.

At this point, note that the strength of ionic interactions and the ion content of ionomers affect the enhancement of the miscibility of ionomer blends strongly. For example, when the interactions between ionic groups generated in an ionomer blend upon the mixing of two non-ionic copolymers are relatively strong, the ionomer blend becomes more homogeneous with increasing ion content. However, at high ion contents, the melt viscosities of the ionomer blends becomes very high, making the processing of the ionomer blends very difficult. In addition, the increasing ion content, naturally, means that the chemical structure and physical nature of ionomers become very different from those of the non-ionic polymers (ie, copolymerization effects). Thus, when the miscibility of the ionomer blends is studied, this copolymerization effect should also be considered carefully. In addition, when the strengths of the ionic interactions of two ionomers are different due to the presence of two different ion pairs, sometimes each ionomer would like to form its own phase-separated regions, thus, leading to immiscible blends. Therefore, the type of ionic interactions and the amount of functional groups should also be taken into account for specific applications of ionomer blends.

5. Plasticization of Ionomers

External plasticizers used for ionomers can be classified into three categories; polar, nonpolar, and amphiphilic plasticizers. These three different types of additives can be used to plasticize either polar or nonpolar regions selectively,

or both regions, depending on the polarities of the additives and the ionomers. In the case of the ionomers, they usually have both polar and nonpolar characteristics (215). Thus, it is possible to plasticize either the ion-rich regions by using a polar plasticizer or the regions of low polarity, ie, the hydrocarbon-rich regions, by using a nonpolar plasticizer. An early study on the dual plasticization is that of Lundberg and co-workers (216). It was found that the ion-rich regions in the SPS ionomers could be plasticized by using a polar plasticizer such as glycerol, which weakened the ionic interactions. As a result, the fast rate of ion hopping occurred, which decreased the cluster T_g, and thus the melt viscosity of the ionomer decreased significantly. It was also found that a nonpolar plasticizer such as dioctylphthalate, interacting with the nonpolar hydrocarbon regions of ionomers, would be distributed more or less evenly throughout both the matrix and cluster regions. Thus, it lowered both the matrix and cluster T_g values. These results imply that the appropriate plasticization is a useful menu for the modification of the thermal behavior of ionomers and the processing methods.

First, attention is turned to the effects of polar plasticizer on ionomer properties. When polar plasticizers are added to ionomers, the plasticizers go into ionic aggregates and cover ionic groups, which reduces the strength of ionic interactions to a point where the ionic groups become relatively mobile. Then, the energy for ion hopping decreases, and thus at relatively low temperatures the ions can move from one multiplet to another at a fast rate. As a result, the cluster T_g shifts to lower temperatures. If the amount of plasticizer were sufficiently large, the multiplets might be shattered completely. At this point, note that the polar plasticizers in ionomers reside not in the nonpolar matrix, but in the multiplets. Thus, the polar plasticization has only little effect on the matrix T_g (216). It was also found that the intensity of a small-angle X-ray scattering peak decreased, and the peak shifted to lower angles upon the addition of methanol to SPS ionomers. As expected, the small-angle X-ray scattering peak disappeared completely at high plasticizer contents (217). This result is expected. The addition of polar plasticizer to the ionic aggregates leads to the increase in the size of the aggregates, which, in turn, decreases the electron density of ionic aggregates. However, when water was added to the Zn-SPS ionomer, it was found that the small-angle X-ray scattering peak shifted to lower angle with increasing peak height (218). Thus, it was suggested that the ionic aggregates were swollen by the water, which induced a rearrangement of ionic groups, leading to the changes in the number of the ionic aggregates and in the fraction of ionic groups that formed ionic aggregates.

Second, the discussion turns to the plasticizers of low polarity such as diethylbenzene or dioctylphthalate. They can be mixed with polymers of low polarity. In the case of styrene ionomers, a nonpolar plasticizer could exist relatively evenly in the cluster and matrix regions because both the two regions consist primarily of nonpolar polystyrene matrix. For example, when the amount of diethylbenzene (DEB) in PSMANa ionomers increased, both the matrix and cluster loss tangent peaks of the ionomers shifted to lower temperatures (219). As expected, the small-angle X-ray scattering peak was found not to change much with the amounts of plasticizer (220). The examples mentioned above lead to the conclusion that while a polar plasticizer would lower the

melt viscosity strongly, it would have little effect on the matrix T_g. The nonpolar plasticizer would lower the melt viscosity slightly, but lower the matrix T_g significantly. In the case of PEA-Na ionomers, having low T_g plasticized with 4-decylaniline (4DA), it was observed that the 4DA was distributed evenly in the cluster and matrix regions through a hydrogen bond between the amine groups of the 4DA and the carbonyl group of the ionomer matrix (221). Thus, the 4DA behaved like a nonpolar plasticizer, and depressed both T_g values nearly in parallel with increasing plasticizer contents. It was also found that as the plasticizer content increased, the intensity of the cluster peak decreased, while that of the matrix peak increased, suggesting that clustered regions were converted into unclustered regions with increasing plasticizer content. In a small-angle X-ray scattering study on the same system, it was found that the spacing between scattering centers increased linearly with increasing weight percentage of 4DA. Thus, it was suggested that the 4DA entered the multiplet regions, resulting in the multiplet swelling. As a result, the spacing increased. In the case of unclustered PMMA ionomer, when 4DA was added to the PMMA ionomer, the 4DA resided in the PMMA matrix phase via a hydrogen bond (101). Thus, the matrix T_g decreased significantly to a point where clustering was induced in the material, making the PMMA ionomer a clustered material. As expected, the unclustered PMMA ionomer, showing no small-angle X-ray scattering peak, started to exhibit a weak small-angle X-ray scattering peak upon plasticization (71). Induced clustering by plasticization can also be found in a poly(styrene-*co*-vinylpyridinium methyl iodide) ionomer system (27). Due to the relatively high matrix T_g and the relatively large size of the ion pairs of the ionomer, the ionomer is unclustered. However, upon the addition of DEB the ionomer becomes clustered and starts shows a small-angle X-ray scattering peak.

Finally, a discussion on amphiphilic plasticizers follows. When zinc stearate was added to zinc sulfonated ethylene–propylene–terpolymer (Zn-EPDM) of very low ion content, some of the Zn stearate might reside in the matrix as microphase separated micelle forms or as highly crystalline regions (222). These phase-separated entities would act as fillers below their melting temperature. Thus, upon the addition of Zn stearate, the matrix T_g and rubbery modulus of the polymer increased slightly. It was also found that the temperature at which the modulus started to drop, presumably associated with the onset of ion hopping, shifted to lower values progressively with increasing the amount of the Zn stearate (222). Above 120°C, a dramatic decrease in the modulus occurred over a narrow temperature range, which might be associated with the melting of the Zn-stearate. In the small-angle X-ray scattering study on the same system, the scattering peak was observed at $q = 1.6\ \text{nm}^{-1}$ ($d_{\text{Bragg}} = 3.9$ nm), and the peak disappeared at temperatures between 115 and 130°C, depending on the amount of the Zn-stearate (32). The small-angle X-ray scattering peak was proposed to correspond to the long period of bilayer crystals of Zn-stearate chains tilted ~27°C. Note that the Zn stearate acted as "multiplet plasticizer" possibly by the incorporation of some carboxylate ionic groups of the Zn stearate into the sulfonate multiplets, which lowered the onset temperature of ion hopping of the ionic groups in the multiplets (222). In addition, at high temperatures the Zn stearate crystalline regions melted, which weakened the strength of ionic interactions. In addition, when an excess amount of Zn stearate was added to

the ionomer, the electron microscopy results revealed that the excess Zn-stearate formed small crystalline regions, with a size of less than ~0.5 μm (223).

In the case of NaSPS ionomers, the matrix T_g decreased only slightly, whereas the cluster T_g dropped significantly upon the addition of a surfactant, sodium dodecylbenzenesulfonate (224,225). In this system, the ionic groups of the surfactant and the ionomer were identical and thought to form multiplets together, and thus the nature of multiplets was not changed by the addition of the surfactant. In addition, the hydrocarbon tails of the surfactant emanating from the multiplet resided in the regions of reduced mobility. Therefore, the surfactant molecules increase the mobility of the polymer chains in the immediate vicinity of the multiplets leading to a decreasing cluster T_g. In the case of para-carboxylated polystyrene ionomer blended with oligomeric styrene-based amphiphiles, it was observed that the plasticization by a styrene oligomer (MW = ~800) terminated with Cs^+ carboxylate was much more effective for the decreasing cluster T_g than that by the oligomer terminated with Ba^{2+} carboxylate (30). When mono- and bifunctional styrene oligomers of a higher molecular weight were used as plasticizers, it was found that both the matrix and cluster phases could be plasticized with monofunctional oligomers. For the ionomers of low ion contents, the bifunctional oligomer showed an antiplasticization effect due to the improved dispersion of the ionic aggregates in the polymer matrix and to the immobilization of the oligomers connected to different multiplets. In the case of the ionomers of high ion contents, however, the oligomer was phase separated because of its much lower ion contents (226). The effects of sodium *p*-toluate and sodium *p*-toluenesulfonate salts on the mechanical properties of styrene-based ionomers were also investigated, and it was found that the organic salt acted both as filler and as plasticizer (12). When a sodium diacid salt was added to the PSMANa ionomer, it was observed that the amphiphilic difunctional salt was distributed in the ionomer matrix and prevented the ionic groups of the ionomer from forming multiplets, causing the decrease in the degree of clustering (227).

From the above examples, one can realize that the plasticization effects on the properties and morphologies of ionomers can be changed drastically by the types of ionomers and plasticizers used. In other words, plasticizer can reside only in multiplets, or exist in the matrix in a well distributed form or as phase-separated filler, or be present in both matrix regions and multiplets, depending on the polarity, crystallinity, and the types of functional groups of plasticizer and ionomer. Thus, the nature of the ionomer and plasticizer can change the plasticization effects significantly.

6. Applications

As expected, ionomers have been used in a wide range of applications. In the 1950s, B.F. Goodrich and DuPont introduced poly(butadiene-*co*-acrylonitrile-*co*-acrylate) elastomers (3) and sulfonated chlorinated polyethylene (Hypalon) (228), respectively, to markets. In the mid-1960s, partially neutralized poly(ethylene-*co*-methacrylate) ionomers (Surlyn) became available in the market by DuPont (1). Since then, substantial studies focused on the synthesis of new

classes of ionomers, new synthetic routes, and new applications have been continued. The aim of this section is to introduce the reader to some of the more interesting applications of ionomers. The particular examples are selected merely to illustrate the very broad range of uses of the ionomers. Since extended abstracts with respect to the ionomer applications appeared in 1988 (229), and several review articles deal with them (230–237), interested readers are referred to the original articles.

6.1. Membranes. One of the most useful applications of ionomer can be found in the ionomer membrane of superpermselectivity (238,239). The most important ionomer for the membrane is PTFE-based ionomers, eg, Nafion, which are copolymers of tetrafluoroethylene and a perfluorinated monomer containing a sulfonate group at the end of a long side chain (240). Since a PTFE matrix is known for its high strength, thermal stability, and chemical stability, the PTFE ionomers find extensive applications in the chlor-alkali industry, in which the PTFE ionomer membranes are used to separate the cathode and anode compartments for the electrolysis process of NaOH from brine (mostly aqueous NaCl solution) (241,242). The use of these membranes saves the cost of electricity considerably, and produces pure NaOH and H_2 on the cathode side and Cl_2 and spent brine on the anode side.

In fuel cells, the conversion of energy generated from chemical reactions into electrical energy takes place; thus, the fuel cells can be used as electric power sources in space crafts and submarines and for the extra electricity needed in new electrical or hybrid automobile applications, such as power batteries, TV, and air conditioning (243,244). The fuel cell consists of anode and cathode compartments, and the compartments are separated by an electrolyte, at which the chemical reactions between H_2 and O_2 (a fuel and an oxidant) occur to produce water and electricity. The electrolyte for fuel cells should be stationary and have high energy efficiency per unit mass and long-term stability. Ionomers as proton exchange membranes can be used as membrane electrolytes (238, 245–247). Especially, perfluorosulfonate ionomers such as Nafion have been widely used as proton conductors because of their high ionic conductivity, good thermal and chemical stability, and satisfactory mechanical strength. However, the high price of Nafion membrane (248) and the environmental hazards at its disposal lead to extensive researches to find the ways to produce other membranes, which are less expensive and more environmentally friendly. In the case of the direct methanol fuel cells (DMFC), they are known to be a good alternative to H_2/air polymer electrolyte fuel cells since they need a simple liquid-fuel handling and show better safety. However, to make the DMFCs available to the market, two technical problems have to be solved. The first problem is the slow kinetics of the oxidative reactions of methanol at the anode. The second problem is methanol diffusion from the anode to the cathode through the Nafion membrane (ie, methanol crossover). Very recently, a number of approaches have been proposed to overcome these two problems, which include the preparation of new ionomer systems and the modification of the operating parameters of the membranes (249–262).

6.2. Molded Materials. Ionomers have found extensive applications as coatings and molded parts, which include golf ball and bowling pin covers, bumper guards and body side molding strips of automobiles, shoe parts, ski

boot shells, and bottle stoppers. Perhaps the most well known use for polyethylene ionomers is golf ball covers (237,238). In general, the high impact resistance and moldability are required for the covers of golf balls having good play characteristics, and the blend of partly neutralized Zn- and Na-EMAA ionomers satisfies these two requirements. The thermoplastic nature of the ionomers allows injection or compression molding applied for the blend to make golf ball covers. In addition, other problems found in ionomers containing single cation (eg, the cold crack in Na-EMAA ionomers and the low rebound in Zn-EMAA ionomer) could be solved effectively and the physical properties of ionomer covers can be tailored by blending both Zn-EMAA and Na-EMAA ionomers and by changing the blend compositions, respectively. Other examples of applications of the ethylene-based ionomers can be found in packaging, impact modifiers, rheology modifiers, modifiers for glass reinforced thermoplastics, ionomer foamed objects, and elastomeric materials. For example, the ionic aggregates in Zn-EPDM elastomeric ionomers act as physical cross-links. Thus, further chemical reaction for the vulcanization of polymers is not required, in contrast to normal elastomers. These ionomers can be used as flexible, waterproof materials such as roofing materials (238,263).

6.3. Fertilizer Coating. Ionomers are also used as a coating for agricultural fertilizers, which improves release properties. Especially, Zn sulfo-EPDM ionomers are used as a coating material for the slow release of fertilizers (264). The volatile polar cosolvent is added to the ionomer solution to plasticize multiplets, which leads to a significant decrease in the solution viscosity. This, in turn, permits easy spraying of ionomer solutions on the spherical urea fertilizers. As the cosolvent and solvent evaporate very rapidly, the aggregation of the ionic groups and the formation of a strong thin film take place. Using this technique, one could obtain various patterns of fertilizer release by changing the size of fertilizer particles and film thickness. When the ionomer-coated urea fertilizers are exposed to water, the water diffuses into the core consisting of urea through the outer ionomer layer, and dissolves the urea particles, resulting in an increase in the osmotic pressure of water inside the coating layer. As the amount of water in the fertilizer cores increases, the pressure on the coating layer increases as well to a point where the cracking of the coating layer occurs. Then, the urea solution is released through the crack of the coating layer. Because of the variation in the thickness of the coating layers, the release of the urea solution takes place over long times. Thus, ionomer-deposition technique on the fertilizer particles allows that the appropriate amount of fertilizers can be released at the height of the growing season, when the fertilizers are most needed.

BIBLIOGRAPHY

"Ionomers" in *ECT* 3rd ed., Suppl. Vol., pp. 546–573, by R. D. Lundberg, Exxon Research and Engineering Co.; in *ECT* 4th ed., Vol. 14, pp. 815–829, by R. W. Rees, E. I. du Pont de Nemours & Co., Inc.; "Ionomers" in *ECT* (online), posting date: December 4, 2000, by R. W. Rees, E. I. du Pont de Nemours & Co., Inc.

1. R. W. Rees and D. J. Vaughan, *Polym. Prepr. (Am. Chem. Soc., Div. Polym. Chem.)* **6**, 287, 296 (1965).
2. A. Eisenberg and M. Rinaudo, *Polym. Bull.* **24**, 671 (1990).
3. H. P. Brown, *Rubber Chem. Technol.* **30**, 1347 (1957).
4. S. Schlick, ed., *Ionomers: Characterization, Theory, and Applications*, CRC Press, Inc., Boca Raton, Fla., 1996.
5. M. R. Tant, K. A. Mauritz, and G. L. Wilkes, eds., *Ionomers: Synthesis, Structure, Properties and Applications*, Blackie Academic Professional, New York, 1996.
6. A. Eisenberg and J.-S. Kim, *Introduction to Ionomers*, John Wiley & Sons, Inc., New York, 1998.
7. A. Eisenberg, H. Farb, and L. G. Cool, *J. Polym. Sci., Part A-2* **4**, 855 (1966).
8. J.-S. Kim, R. J. Jackman, and A. Eisenberg, *Macromolecules* **27**, 2789 (1994).
9. A. Eisenberg, B. Hird, and R. B. Moore, *Macromolecules* **23**, 4098 (1990).
10. B. Hird and A. Eisenberg, *Macromolecules* **25**, 6466 (1992).
11. B. Hird and A. Eisenberg, *J. Polym. Sci.: Part B: Polym. Phys.* **28**, 1665 (1990).
12. Y. H. Nah and co-workers, *Polym. J.* **31**, 309 (1999).
13. W. Y. Hsu, J. R. Barkley, and P. Meakin, *Macromolecules* **13**, 198 (1980).
14. H. Ukihashi and M. Yamabe, in A. Eisenberg and H. L. Yeager, eds., *Perfluorinated Ionomer Membranes*, ACS Symposium Series 180, American Chemical Society, Washington, D.C., 1982, Chapt. 17.
15. A. A. Gronowski and co-workers, *J. Membr. Sci.* **82**, 83 (1993).
16. M. Jiang and co-workers, *Macromolecules* **27**, 6541 (1994).
17. R. D. Lundberg and H. S. Markowski, in A. Eisenberg, ed., *Ions in Polymers* (Advances in Chemistry Series 187), American Chemical Society, Washington, D.C., 1980, Chapt. 2.
18. A. Eisenberg, *Macromolecules* **3**, 147 (1970).
19. F. C. Wilson, R. Longworth, and D. J. Vaughan, *Polym. Prepr. (Am. Chem. Soc., Div. Polym. Chem.)* **9**, 505 (1968).
20. R. Longworth and D. J. Vaughan *, Nature (London)* **218**, 85 (1968).
21. C. L. Marx, D. F. Caulfield, and S. L. Cooper, *Macromolecules* **6**, 344 (1973).
22. M. Pineri and co-workers, *J. Polym. Sci., Polym. Phys. Ed.* **12**, 115 (1974).
23. W. J. MacKnight, W. P. Taggart, and R. S. Stein, *J. Polym. Sci., Polym. Symp.* **45**, 113 (1974).
24. ??????????
25. D. J. Yarusso and S. L. Cooper, *Macromolecules* **16**, 1871 (1983); *Polymer* **26**, 371 (1985).
26. R. B. Moore and co-workers, *Macromolecules* **24**, 1376 (1991).
27. D. Wollmann, C. E. Williams, and A. Eisenberg, *Macromolecules* **25**, 6775 (1992).
28. H. Tomita and R. A. Register, *Macromolecules* **26**, 2791 (1993).
29. T. Hashimoto and co-workers, *Polymer* **35**, 2672 (1994).
30. M. Plante, C. G. Bazuin, and R. Jérôme, *Macromolecules* **28**, 1567 (1995).
31. X. Lu and co-workers, *Macromolecules* **28**, 2831 (1995).
32. D. A. Jackson, J. T. Koberstein, and R. A. Weiss, *J. Polym. Sci.: Part B: Polym. Phys.* **37**, 3141 (1999).
33. K. Suchocka-Galas, C. Slusarczyk, and A. Wlochowicz, *Eur. Polym. J.* **36**, 2167, 2175 (2002).
34. P. Y. Vuillaume, C. G. Bazuin, and J.-C. Galin, *Macromolecules* **33**, 781 (2000).
35. S. Kutsumizu and co-workers, *Macromolecules* **33**, 3818 (2000).
36. R. F. Storey and D. W. Baugh, III, *Polymer* **41**, 3205 (2000).
37. P. Y. Vuillaume, J.-C. Galin, and C. G. Bazuin, *Macromolecules* **34**, 859 (2001).
38. Y. Tsujita and co-workers, *Macromolecules* **34**, 2220 (2001).
39. Y. Tsujita and co-workers, *J. Polym. Sci.: Part B: Polym. Phys.* **40**, 831 (2002).

40. S. Kutsumizu and co-workers, *Macromolecules* **35**, 6298 (2002).
41. C. T. Meyer and M. Pineri, *J. Polym. Sci., Polym. Phys. Ed.* **16**, 569 (1978).
42. E. J. Roche and co-workers, *J. Polym. Sci., Polym. Phys. Ed.* **19**, 1 (1981).
43. T. R. Earnest, J. S. Higgins, and W. J. MacKnight, *Macromolecules* **15**, 1390 (1982).
44. G. Gebel and J. Lambard, *Macromolecules* **30**, 7914 (1997).
45. G. Gebel, *Polymer* **41**, 5829 (2000).
46. G. Gebel and R. B. Moore, *Macromolecules* **33**, 4850 (2000).
47. Y. S. Ding and co-workers, *J. Appl. Phys.* **56**, 2396 (1984).
48. D. J. Yarusso and co-workers, *J. Polym. Sci., Polym. Phys. Ed.* **22**, 2073 (1984).
49. A. Meagher and co-workers, *Polymer* **27**, 979 (1986).
50. G. Vlaic and co-workers, *Polymer* **29**, 173 (1988).
51. B. P. Grady, *Macromolecules* **32**, 2983 (1999).
52. A. Welty, S. Ooi, and B. P. Grady, *Macromolecules* **32**, 2989 (1999).
53. B. P. Grady, *Polymer* **41**, 2325 (2000).
54. K. V. Farrell and B. P. Grady, *Macromolecules* **34**, 7 (2001).
55. D. L. Handlin, W. J. MacKnight, and E. L. Thomas, *Macromolecules* **14**, 795 (1981).
56. C. Li, R. A. Register, and S. L. Cooper, *Polymer* **30**, 1227 (1989).
57. J. H. Laurer and K. Winey, *Macromolecules* **31**, 9106 (1998).
58. K. I. Winey, J. H. Laurer, and B. P. Kirkmeyer, *Macromolecules* **33**, 507 (2000).
59. B. P. Kirkmeyer, R. A. Weiss, and K. I. Winey, *J. Polym. Sci.: Part B: Polym. Phys.* **39**, 477 (2001).
60. B. P. Kirkmeyer and co-workers, *Macromolecules* **35**, 2648 (2002).
61. A. Taubert and K. I. Winey, *Macromolecules* **35**, 7419 (2002).
62. M. Moffitt, K. Khougaz, and A. Eisenberg, *Acc. Chem. Res.* **29**, 95 (1996).
63. S. E. Webber, P. Munk, and Z. Tuzar, eds., *Solvents and Self-Organization of Polymers*, Kluwer Academic Publishers, Dordrecht, The Netherlands, 1996.
64. N. S. Cameron, M. K. Corierre, and A. Eisenberg, *Can. J. Chem.* **77**, 1311 (1999).
65. N. M. Benetatos, H. Kim, and K. I. Winey, MRS 2004 Fall Meeting Abstracts 657 (2004).
66. A. Lehmani, S. Durand-Vidal, and P. Turq, *J. Appl. Polym. Sci.* **68**, 503 (1998).
67. P. J. James and co-workers, *Polymer* **41**, 4223 (2000).
68. R. S. McLean, M. Doyle, and B. B. Sauer, *Macromolecules* **33**, 6541 (2000).
69. B. B. Sauer and R. S. McLean, *Macromolecules* **33**, 7939 (2000).
70. S.-H. Kim and J.-S. Kim, *Macromolecules* **36**, 2382 (2003).
71. J.-S. Kim and A. Eisenberg, *Polym. J.* **31**, 303 (1999).
72. K. J. Liu and J. E. Anderson, *Macromolecules* **2**, 235 (1969).
73. J.-S. Kim, M.-C. Hong, and Y. H. Nah, *Macromolecules* **35**, 155 (2002).
74. S.-H. Kim and J.-S. Kim, *Macromolecules* **36**, 1870 (2003).
75. J. A. Lefelar and R. A. Weiss, *Macromolecules* **17**, 1145 (1984).
76. I. A. Nyrkova, A. R. Khokhlov, and M. Doi, *Macromolecules* **26**, 3601 (1993).
77. S. Yano, K. Tadano, and R. Jérôme, *Macromolecules* **24**, 6439 (1991).
78. S. Yano and co-workers, *Macromolecules* **25**, 368 (1992).
79. S. Kutsumizu and co-workers, *Macromolecules* **26**, 752 (1993).
80. Z. Gao, X.-F. Zhong, and A. Eisenberg, *Macromolecules* **27**, 794 (1994).
81. P. Vanhoorne and co-workers, *Macromolecules* **27**, 2548 (1994).
82. G. Tsagaropoulos and A. Eisenberg, *Macromolecules* **28**, 6067 (1995).
83. G. Tsagaropoulos, J.-S. Kim, and A. Eisenberg, *Macromolecules* **29**, 2222 (1996).
84. B. Grassl and co-workers, *Macromolecules* **30**, 236 (1997).
85. S. Kutsumizu and S. Schlick, *Macromolecules* **30**, 2329 (1997).
86. S. Kutsumizu, M. Goto, and S. Yano, *Macromolecules* **37**, 4821 (2004).
87. J.-S. Kim, G. Wu, and A. Eisenberg, *Macromolecules* **27**, 814 (1994).
88. J. Kim and J.-S. Kim, *Polym. Bull.* **46**, 403 (2001).

89. T. Kanamoto and co-workers, *Makromol. Chem.* **176**, 3497 (1975).
90. J. J. Maurer, in B. Miller, ed., *Thermal Analysis: Proceedings of the Seventh International Conference on Thermal Analysis*, Vol 2, John Wiley & Sons, Inc., New York, 1982, pp. 1040–1049.
91. X. Tong and C. G. Bazuin, *Chem. Mater.* **4**, 370 (1992).
92. M. Ehmann and co-workers, *Macromolecules* **26**, 4910 (1993).
93. T. Takamatsu and A. Eisenberg, *J. Appl. Polym. Sci.* **24**, 2221 (1979).
94. W. J. MacKnight, L. W. McKenna, and B. E. Read, *J. Appl. Phys.* **38**, 4208 (1967).
95. E. P. Otocka and T. K. Kwei, *Macromolecules* **1**, 401 (1968).
96. A. Eisenberg and M. Navratil, *Macromolecules* **6**, 604 (1973).
97. R. A. Weiss, P. K. Agarwal, and R. D. Lundberg, *J. Appl. Polym. Sci.* **29**, 2719 (1984).
98. D. Wollman, S. Gauthier, and A. Eisenberg, *Polym. Eng. Sci.* **26**, 1451 (1986).
99. T. C. Ward and A. V. Tobolsky, *J. Appl. Polym. Sci.* **11**, 2403 (1967).
100. M. Hara and co-workers, in A. Eisenberg and F. E. Bailey, eds., *Coulombic Interactions in Macromolecular Systems*, ACS Symposium Series 302, American Chemical Society, Washington, D.C., 1986, Chapt. 14.
101. N. K. Tierney and R. A. Register, *Macromolecules* **35**, 2358 (2002).
102. M. Rigdahl and A. Eisenberg, *J. Polym. Sci., Polym. Phys. Ed.* **19**, 1641 (1981).
103. J.-S. Kim, K. Yoshikawa, and A. Eisenberg, *Macromolecules* **27**, 6347 (1994).
104. S. Gauthier, D. Duchesne, and A. Eisenberg, *Macromolecules* **20**, 753 (1987).
105. J.-S. Kim, H.-S. Kim, and A. Eisenberg, *Bull. Korean Chem. Soc.* **19**, 623 (1998).
106. H.-S. Kim and co-workers, *Polym. J.* **31**, 306 (1999).
107. A. Eisenberg, in J. E. Mark and co-workers, *Physical Properties of Polymers*, ACS Professional Reference Book, American Chemical Society, Washington, D.C., 1993, Chapt. 2.
108. A. Eisenberg and M. Navratil, *Macromolecules* **6**, 604 (1973).
109. R. D. Lundberg and R. R. Phillips, *J. Polym. Sci.: Polym. Lett. Ed.* **22**, 377 (1984).
110. R. Longworth and D. J. Vaughan, *Polym. Prepr. (Am. Chem. Soc., Polym. Chem. Div.)* **9**, 525 (1968).
111. K. Tadano and co-workers, *Macromolecules* **22**, 226 (1989).
112. H. Tachino and co-workers, *Macromolecules* **26**, 752 (1993).
113. H. Tachino and co-workers, *Macromolecules* **27**, 372 (1994).
114. P. Vanhoorne and R. A. Register, *Macromolecules* **29**, 598 (1996).
115. H. Hashimoto and co-workers, *Macromolecules* **34**, 1515 (2001).
116. S. C. Yeo and A. Eisenberg, *J. Appl. Polym. Sci.* **21**, 875 (1977).
117. I. M. Hodge and A. Eisenberg, *Macromolecules* **11**, 289 (1978).
118. T. Kyu and A. Eisenberg , in Ref. 14, Chapt. 6.
119. T. Kyu, M. Hashiyama, and A. Eisenberg, *Can. J. Chem.* **61**, 680 (1983).
120. T. Kyu and A. Eisenberg, *J. Polym. Sci., Polym. Symp.* **71**, 203 (1984).
121. Y. Nakano and W. J. MacKnight, *Macromolecules* **17**, 1585 (1984).
122. S. Gauthier and A. Eisenberg, *Macromolecules* **20**, 760 (1987).
123. T. E. Long, R. D. Allen, and J. E. McGrath, in J. L. Benham and J. F. Kinstel, eds., *Chemical Reaction on Polymers*, ACS Symposium Series 364, American Chemical Society, Washington, D.C., 1988, Chapt. 19.
124. R. A. Weiss and co-workers, *Polymer* **32**, 2785 (1991).
125. A. Desjardins and A. Eisenberg, *Plast. Rubber Compos. Process. Appl.* **18**, 161 (1992).
126. K. Yoshikawa and co-workers, *Macromolecules* **29**, 1235 (1996).
127. G. Broze and co-workers, *J. Polym. Sci., Polym. Phys. Ed.* **21**, 2205 (1983).
128. R. Jérôme and G. Broze, *Rubber Chem. Technol.* **58**, 223 (1984).
129. G. Broze, R. Jérôme, and Ph. Teyssié, in P. Dubin, ed., *Polymer Science and Technology*, Vol. 30, Plenum Press, New York, 1985.

130. R. Jérôme, in E. Goethals, ed., *Telechelic Polymers: Synthesis and Applications*, CRC Press, Inc., Boca Raton, Fla., 1989, Chapt. 11.
131. P. Charlier, R. Jérôme, Ph. Teyssié, and L. A. Utracki, *Macromolecules* **25**, 617 (1992).
132. P. Vanhoorne and R. Jérôme, in Ref.4 , Chapt. 9.
133. Y. Mohajer and co-workers, *Polym. Bull.* **8**, 47 (1982).
134. S. Bagrodia and co-workers, *Polym. Bull.* **9**, 174 (1983).
135. Y. Mohajer and co-workers, *J. Appl. Polym. Sci.* **29**, 1943 (1984).
136. S. Bagrodia and co-workers, *Polymer* **28**, 2207 (1987).
137. D. Loveday and co-workers, *J. Appl. Polym. Sci.* **63**, 507 (1997).
138. R. F. Storey, B. J. Chisholm, and Y. Lee, *Polym. Eng. Sci.* **37**, 73 (1997).
139. M. Rutkowska and R. Zielinski, in M. Pineri and A. Eisenberg, eds., *Structure and Properties of Ionomers*, NATO ASI Series C: Mathematical and Physical Sciences, Vol. 198, D. Reidel Publishing Co., Dordrecht, The Netherlands, 1987, pp. 469–479.
140. S. A. Visser and S. L. Cooper, *Macromolecules* **24**, 2576 (1991).
141. H. X. Xiao and K. C. Frisch, eds., *Advances in Urethane Ionomers*, Technomic Publishing Company, Inc., Lancaster, Pa., 1995.
142. A. Eisenberg, H. Matsuura, and T. Yokoyama, *Polym. J.* **2**, 117 (1971).
143. D. Feng and co-workers, *Polymer* **33**, 526 (1992).
144. T. Tsutsui, in A. D. Wilson, ed., *Development in Ionic Polymers-2*, Elsevier, New York, 1980, Chapt. 4.
145. C. G. Bazuin and co-workers, *Polymer* **30**, 654 (1989).
146. M. Ehrmann, R. Muller, J.-C. Galin, and C. G. Bazuin, *Macromolecules* **26**, 4910 (1993).
147. H. Matuura and A. Eisenberg, *J. Polym. Sci., Polym. Phys. Ed.* **14**, 1201 (1976).
148. X. Tong and C. G. Bazuin, *Chem. Mater.* **4**, 370 (1992).
149. J.-S. Kim, Y. H. Nah, and S. S. Jahng, *Polymer* **42**, 5567 (2001).
150. A. A. Gronowski and co-workers, *J. Membr. Sci.* **82**, 83 (1993).
151. X. Ma, J. A. Sauer, and M. Hara, *Macromolecules* **28**, 3953 (1995); *Polymer* **38**, 4425 (1997).
152. B. Zhang and R. A. Weiss, *J. Polym. Sci.: Part A: Polym. Chem.* **30**, 91 (1992).
153. C. G. Bazuin and A. Tork, *Macromolecules* **28**, 8877 (1995).
154. Y. Xue and M. Hara, *Macromolecules* **30**, 3803 (1997).
155. C. Chovino and co-workers *J. Polym. Sci.: Part A: Polym. Chem.*, **35**, 2569 (1997).
156. J.-F. Gohy and co-workers, *Macromol. Chem. Phys.* **199**, 1791 (1998).
157. E. Barmatov and co-workers, *Macromol. Rapid Commun.* **21**, 281 (2000).
158. E. B. Barmatov and co-workers, *Macromolecules* **37**, 5490 (2004).
159. R. D. Lundberg, in Ref. 136, pp. 387–397.
160. C. W. Lantman, W. J. MacKnight, and R. D. Lundberg, *Annu. Rev. Mater. Sci.* **295**, 19 (1989).
161. M. Hara, in M. Hara, ed., *Polyelectrolytes: Science and Technology*, Marcel Dekker, Inc., New York, 1993, Chapt. 4.
162. M. Hara, in J. C. Salamone, ed., *Polymeric Materials Encyclopedia*, Vol. 5, CRC Press, Inc., Boca Raton, Fla., 1996, pp. 3473–3481.
163. D. R. Paul and S. Newman, eds., *Polymer Blends*, Academic Press, New York, 1978.
164. O. Olabisi, L. M. Robeson, and M. T. Shaw, *Polymer–Polymer Miscibility*, Academic Press, New York, 1979.
165. L. A. Utracki, *Polymer Alloys and Blends: Thermodynamics and Rheology*, Hanser Publishers, Munich, 1989.
166. L. A. Utracki, in R. A. Weiss, ed., *Multiphase Polymers: Blends and Ionomers*, ACS Symposium Series 395, American Chemical Society, Washington, D.C., 1989.
167. A. Y. Coran, R. Patel, and D. Williams-Head, *Rubber Chem. Technol.* **58**, 1014 (1985).

168. B. A. Thornton, R. G. Villasenor, and B. Maxwell, *J. Appl. Polym. Sci.* **25**, 653 (1980).
169. N. Yoshimura and K. Fujimoto, *Rubber Chem. Technol.* **42**, 1009 (1969).
170. L. H. Sperling and co-workers, *J. Appl. Polym. Sci.* **14**, 73 (1970).
171. K. L. Smith, A. E. Winslow, and D. E. Petersen, *Ind. Eng. Chem.* **48**, 1361 (1959).
172. L. M. Robeson and J. E. McGrath, *Polym. Eng. Sci.* **17**, 300 (1977).
173. N. E. Weeks, F. E. Karasz, and W. J. MacKnight, *J. Appl. Phys.* **48**, 4068 (1977).
174. S. F. Fahrenholtz and T. K. Kwei, *Macromolecules* **14**, 1076 (1981).
175. E. M. Pearce, T. K. Kwei, and B. Y. Min, *J. Macromol. Sci., Chem.* **A21**, 1181 (1984).
176. R. E. Taylor-Smith and R. A. Register, *Macromolecules* **26**, 2802 (1993).
177. R. E. Taylor-Smith and R. A. Register, *J. Polym. Sci.: Part B: Polym. Phys.* **32**, 2105 (1994).
178. S. W. Kuo and F. C. Chang, *Macromolecules* **34**, 7737 (2001).
179. A. S. Michaels, *Ind. Eng. Chem.* **57**, 32 (1968).
180. R. E. Prud'homme, *Polym. Eng. Sci.* **22**, 90 (1982).
181. D. Allard and R. E. Prud'homme, *J. Appl. Polym. Sci.* **27**, 559 (1982).
182. G. Belorgey, M. Aubin, and R. E. Prud'homme, *Polymer* **23**, 1051 (1982).
183. M. B. Djordjevic and R. S. Porter, *Polym. Eng. Sci.* **23**, 650 (1983).
184. C. Pugh and V. Percec, *Macromolecules* **19**, 65 (1986).
185. T. Sulzberg and R. J. Cotter, *J. Polym. Sci., Part A-1* **8**, 2747 (1970).
186. N. Ohno and J. Kumanotani, *Polym. J.* **11**, 947 (1979).
187. K. Abe and co-workers, *Makromol. Chem.* **186**, 1505 (1985).
188. S. Alexandra and A. Nathansohn, *Macromolecules* **23**, 5127 (1990).
189. A. S. Michaels and R. G. Miekka, *J. Phys. Chem.* **65**, 1765 (1961).
190. V. A. Kabanov, *Pure Appl. Chem. Macromol. Chem.* **8**, 121 (1983).
191. M. Lysaght, in K. C. Fisch, D. Klempner, and A. V. Patsis, eds., *Polyelectrolytes*, Technomic Publishing Co., Inc., Westport, 1975, pp. 34–42.
192. E. Tsuchida and K. Abe, *Adv. Polym. Sci.* **45**, 1 (1982).
193. V. A. Kabanov and A. B. Zezin, *Makromol. Chem., Suppl.* **6**, 259 (1984).
194. Y. Li, J. Xia, and P. L. Dubin, *Macromolecules* **27**, 7049 (1994).
195. Y. Li and co-workers, *Macromolecules* **28**, 3098 (1995).
196. P. Smith, M. Hara, and A. Eisenberg, in R. M. Ottenbrite, L. A. Utracki, and S. Inoue, eds., *Current Topics in Polymer Science*, Vol. 2, Hanser Publisher, New York, 1987, pp. 256–283.
197. A. Natansohn, R. Murali, and A. Eisenberg, *Makromol. Chem. Macromol. Symp.* **16**, 175 (1988).
198. Z. Gao, A. Molnár, and A. Eisenberg, in Ref. 5, Chapt. 10.
199. C. G. Bazuin, in Ref. 158, pp. 3454–3460.
200. E. P. Otocka and F. R. Eirich, *J. Polym. Sci., A-2* **6**, 921 (1968).
201. X. Zhang and A. Eisenberg, *Polym. Adv. Technol.* **1**, 9 (1990).
202. X. Zhang and A. Eisenberg, *J. Polym. Sci.: Part B: Polym. Phys.* **28**, 1841 (1990).
203. P. Smith and A. Eisenberg, *J. Polym. Sci.: Polym. Lett. Ed.* **21**, 223 (1983).
204. B. Vollmert and W. Schoene, in G. E. Molau, ed., *Colloidal and Morphological Behavior of Block and Graft Copolymers*, Plenum, Inc., New York, 1977, pp. 145–157.
205. M. Rutkowska and A. Eisenberg, *J. Appl. Polym. Sci.* **30**, 3317 (1985).
206. M. Hara and A. Eisenberg, *Macromolecules* **17**, 1335 (1984).
207. M. J. Sullivan and R. A. Weiss, *Polym. Eng. Sci.* **32**, 517 (1992).
208. A. Molnár and A. Eisenberg, *Macromolecules* **25**, 5774 (1992).
209. X. Lu and R. A. Weiss, *Macromolecules* **25**, 6185 (1992).
210. C.-W. A. Ng, M. A. Bellinger, and W. J. MacKnight, *Macromolecules* **27**, 6942 (1994).
211. J.-H. Lim, J.-K. Park, and H.-Y. Song, *J. Polym. Sci.: Part B: Polym. Phys.* **32**, 29 (1994).
212. D. G. Peiffer and co-workers, *J. Polym. Sci., Polym. Lett. Ed.* **24**, 581 (1986).

213. K. Sakurai, E. Douglas, and W. J. MacKnight, *Macromolecules* **26**, 208 (1993).
214. E. P. Douglas, A. J. Waddon, and W. J. MacKnight, *Macromolecules* **27**, 4344 (1994).
215. C. G. Bazuin, in Ref. 158, pp. 3454–3460.
216. R. D. Lundberg, H. S. Makowski, and L. Westerman, in Ref. 16, Chapt. 3.
217. J. J. Fitzgerald and R. A. Weiss, *J. Polym. Sci.: Part B: Polym. Phys.* **28**, 1719 (1990).
218. D. J. Yarusso and S. L. Cooper, *Polymer* **26**, 371 (1985).
219. C. G. Bazuin and A. Eisenberg, *J. Polym. Sci.: Part B: Polym. Phys.* **24**, 1137 (1986).
220. R. A. Weiss, J. J. Fitzgerald, and D. Kim, *Macromolecules* **24**, 1064 (1991).
221. X. Tong and C. G. Bazuin, *J. Polym. Sci.: Part B: Polym. Phys.* **30**, 389 (1992).
222. P. K. Agarwal, H. S. Makowski, and R. D. Lundberg, *Macromolecules* **13**, 1679 (1980).
223. S. K. Ghosh and co-workers, *J. Appl. Polym. Sci.* **78**, 743 (2000).
224. I. Duvdevani and co-workers, in Ref. 101, Chapt. 15.
225. J.-S. Kim and co-workers, *Macromolecules* **26**, 5256 (1993).
226. M. Plante, C. G. Bazuin, and R. Jérôme, *Macromolecules* **28**, 5240 (1995).
227. J.-W. Kim, J.-S. Kim, and S.-S. Jarng, *Polymer* **44**, 2993 (2003).
228. R. R. Warner, *Rubber Age* **71**, 2 (1952).
229. Extended abstracts [in *Polym. Prepr. (Am. Chem. Soc., Div. Polym. Chem.)* **29**, pp. 429–445 (1988)].
230. R. H. Kinsey, *Appl. Polym. Symp.* **11**, 77 (1969).
231. R. A. Weiss and co-workers, in Ref. 101, Chapt. 1.
232. W. J. MacKnight, in Ref.136 , pp. 1–9.
233. R. D. Lundberg, in Ref. 136, pp. 279–290.
234. R. D. Lundberg, in Ref. 136, pp. 429–438.
235. J. S. Tan, in Ref. 136, pp. 439–451.
236. R. D. Lundberg, in J. I. Kroschwitz, ed., *Encyclopedia of Polymer Science and Engineering*, Vol. 8, John Wiley & Sons, Inc., New York, 1987, pp. 393–423.
237. R. J. Statz, *Polym. Prepr. (Am. Chem. Soc., Div. Polym. Chem.)* **29**, 435 (1988).
238. W. M. Risen, Jr., in Ref. 4, Chapt. 12.
239. A. Eisenberg and H. L. Yeager, eds., *Perfluorinated Ionomer Membranes*, ACS Symposium Series 180, American Chemical Society, Washington, D.C., 1982.
240. K. A. Mauritz and R. B. Moore, *Chem. Rev.* **104**, 4535 (2004).
241. W. G. F. Grot, *Chim. Ing. Tech.* **50**, 299 (1978).
242. E. I. Baucom, *Mod. Chlor Alkali Technol.* **5**, 131 (1992).
243. H. Voss and J. Huff, *J. Power Source* **65**, 155 (1997).
244. A. Heinzel and co-workers, *Electrochim. Acta* **43**, 3817 (1998).
245. H. L. Yeager and A. A. Gronowski, in Ref. 5, Chapt. 8.
246. O. Savadogo, *J. New Mater. Electrochem. Syst.* **1**, 47 (1998).
247. K. D. Kreuer, *J. Membr. Sci.* **185**, 29 (2001).
248. A. J. Appleby and F. R. Foulkes, *Fuel Cell Handbook*, Van Nostrand Reinhold, New York, 1989, p. 762.
249. C. Bailly and co-workers, *Polymer* **28**, 1009 (1987).
250. R. Nolte and co-workers, *J. Membr. Sci.* **83**, 211 (1993).
251. B. Gupta, F. N. Buchi, and G. Scherer, *J. Polym. Sci.: Part A: Polym. Chem.* **32**, 1931 (1994).
252. J. T. Wang and co-workers, *J. Appl. Electrochem.* **26**, 751 (1996).
253. B. S. Pivovar, Y. Wang, and E. L. Cussler, *J. Membr. Sci.* **154**, 155 (1999).
254. A. Heinzel and V. M. Barragán, *J. Power Sources* **84**, 70 (1999).
255. D. Riven and co-workers, *Polymer* **42**, 623 (2001).
256. P. D. Beatie and co-workers, *J. Electroanal. Chem.* **503**, 45 (2001).
257. P. Genova-Dimitrova and co-workers, *J. Membr. Sci.* **185**, 59 (2001).
258. J. Kim, B. Kim, and B. Jung, *J. Membr. Sci.* **207**, 129 (2002).

259. L. J. Hobson and co-workers, *J. Power Sources* **104**, 79 (2002).
260. M. V. Fedkin and co-workers, *Mater. Lett.* **52**, 192 (2002).
261. P. Mukoma, B. R. Jooste, and H. C. M. Vosloo, *J. Membr. Sci.* **243**, 293 (2004).
262. Y. S. Kim and co-workers, *J. Membr. Sci.* **243**, 317 (2004).
263. A. U. Paeglis and F. X. O'Shea, *Rubber Chem. Technol.* **61**, 223 (1988).
264. E. N. Drake, *Polym. Mater. Sci. Eng.* **71**, 14 (1994).

JOON-SEOP KIM
Department of Polymer Science
& Engineering, Chosun University

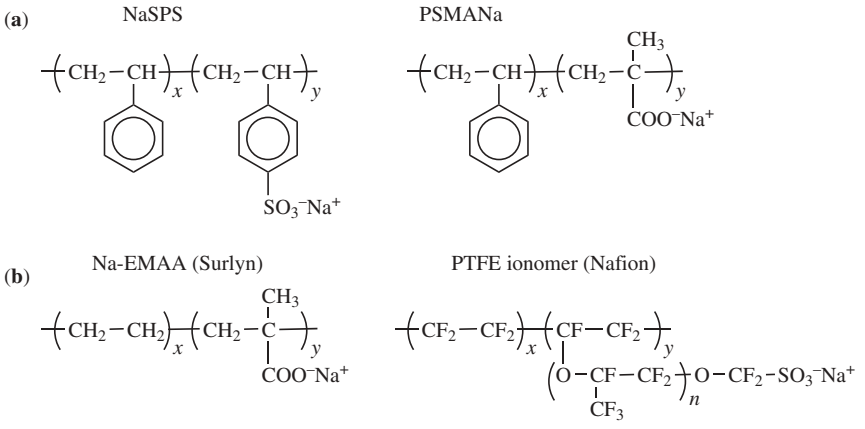

Fig. 1. (**a**) Amorphous ionomers. (**b**) Crystalline ionomers.

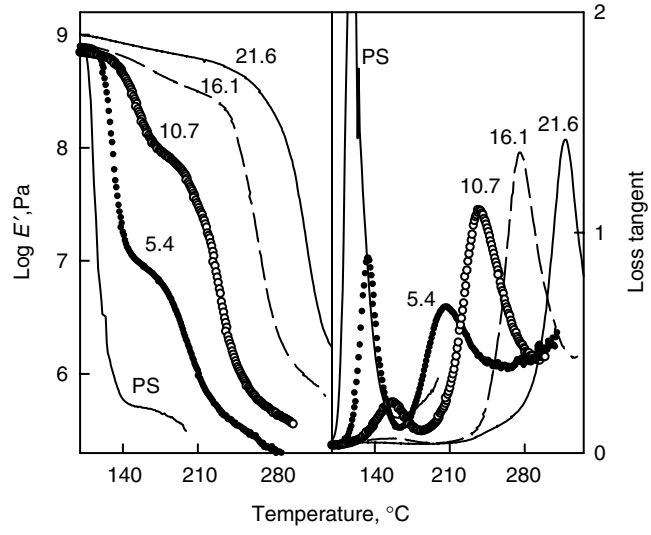

Fig. 2. Storage moduli (E') and loss tangent measured at 1 Hz as a function of temperature for PSMANa ionomers with ion contents marked near each plot (data were obtained from Ref. 8).

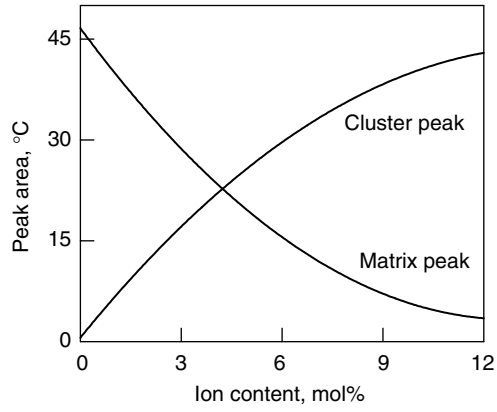

Fig. 3. Area under loss tangent peaks of PSMANa ionomers as a function of ion content, measured at 1 Hz (modified from Ref. 8).

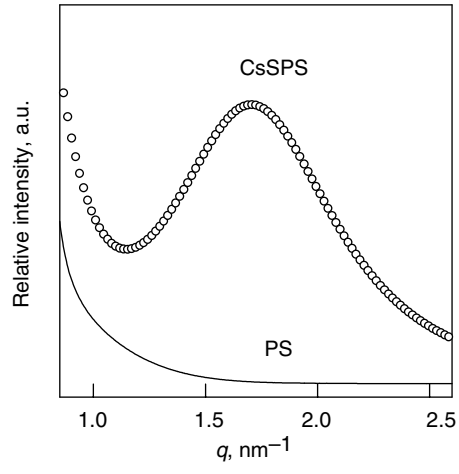

Fig. 4. Small-angle X-ray scattering data as a function of $q(=4\pi\sin\theta/\lambda$, θ is one-half of the scattering angle and λ is the X-ray wavelength) for polystyrene and poly (styrene-*co*-cesium styrenesulfonate) (CsSPS) ionomer containing 7.7 mol% of ions.

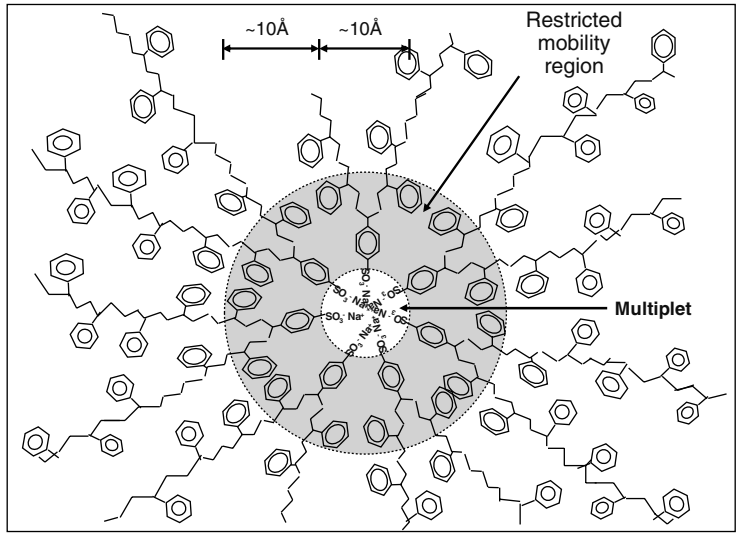

Fig. 5. Representative scheme of a multiplet and of the region of restricted mobility surrounding it in a poly(styrene-*co*-sodium styrenesulfonate) ionomer.

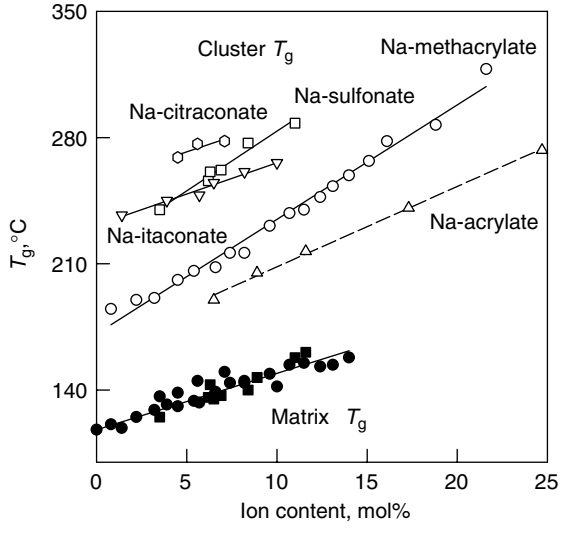

Fig. 6. Glass-transition temperatures of matrix and cluster regions versus ion content for sodium neutralized poly(styrene-*co*-methacrylate), poly(styrene-*co*-acrylate), poly-(styrene-*co*-styrenesulfonate), poly(styrene-*co*-itaconate), and poly(styrene-*co*-citraconate) ionomers (some of data were obtained from Refs. 8,10,73,87, and 88).

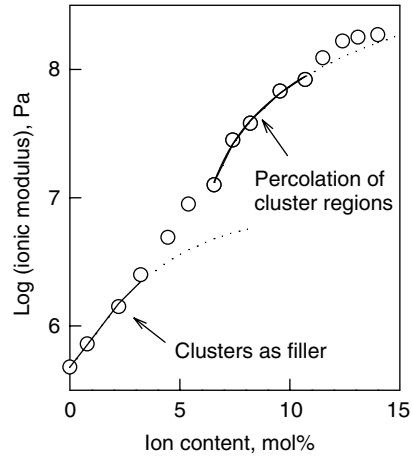

Fig. 7. Log of the ionic modulus (1 Hz) versus ion content for PSMANa ionomers of various ion contents. Points: experimental; lines calculated from filler and percolation approaches.

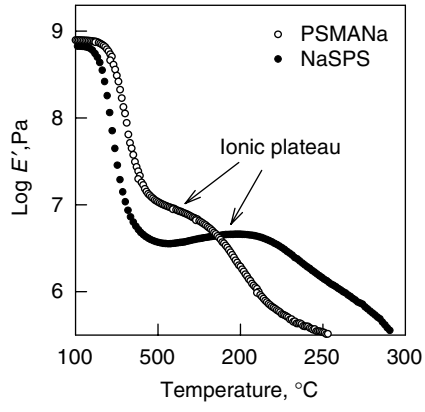

Fig. 8. Storage moduli (E') measured at 1 Hz as a function of temperature for PSMANa and Na-SPS ionomers containing 5.4 and 5.1 mol% of ions, respectively.

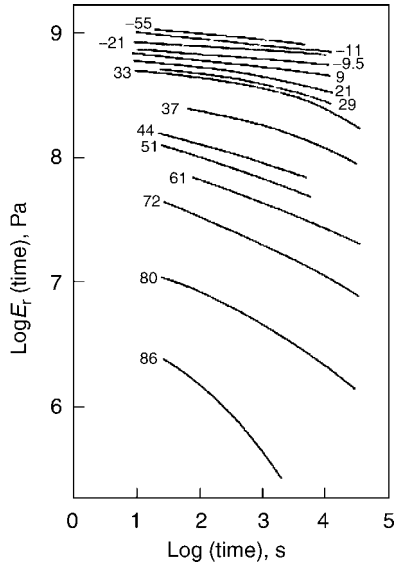

Fig. 9. Stress relaxation curves for an annealed poly(ethylene-*co*-methacrylate) ionomer containing 8 mol% of acid groups, 47% of which were neutralized with NaOH (modified from Ref. 99).

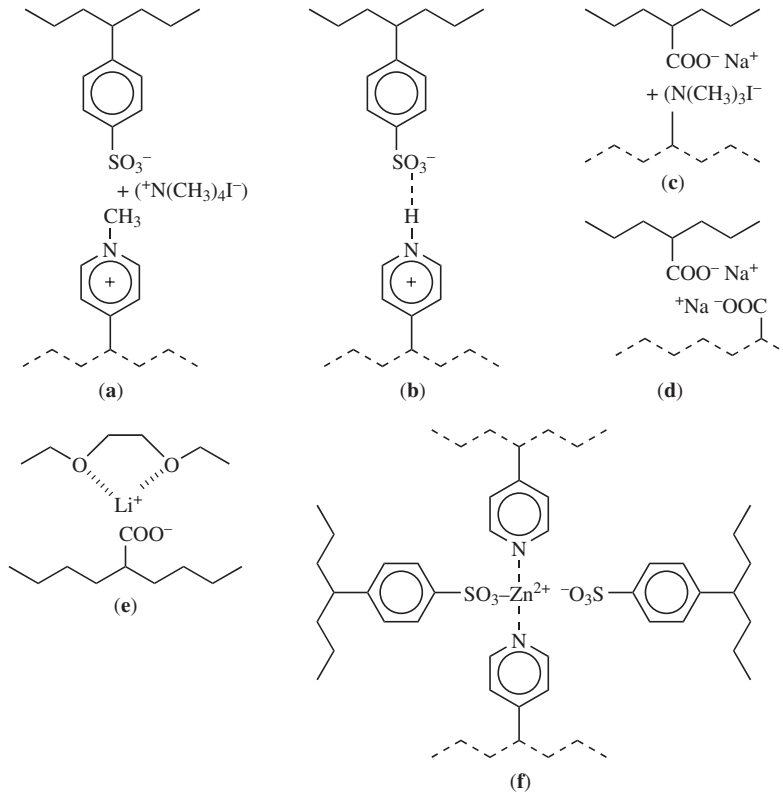

Fig. 10. Menu of ionic interactions leading to miscibility enhancement. (**a**) ion–ion, (**b**) hydrogen bond assisted ion–ion, (**c**) complementary ion pair–ion pair, (**d**) identical ion pair–ion pair, (**e**) ion–dipole, and (**f**) ion coordination.